PERGAMON

Vacuum 68 (2003) 79–85

VACUUM
SURFACE ENGINEERING, SURFACE INSTRUMENTATION & VACUUM TECHNOLOGY

www.elsevier.com/locate/vacuum

Application of carbon nanotubes to the cathode ray tube-electron gun

Yoon-Taek Jang[a,*], Yun-Hi Lee[a], Byeong-Kwon Ju[a], Jin-Ho Ahn[b], Chang-Ki Go[c], Gong-Seog Park[c]

[a] *Nano Devices and Physics Laboratory, Korea Institute of Science and Technology, P.O. Box 131, Cheongryang, Seoul, South Korea*
[b] *Division of Materials Science & Engineering, Hanyang University Korea, South Korea*
[c] *LG Electronics Inc., Kumi, South Korea*

Received 17 December 2001; accepted 21 February 2002

Abstract

We present fabrication of the carbon nanotubes (CNTs) electron guns for the cathode ray tubes (CRT) and their electron emission properties as well as light emitting characteristics. The CNTs were grown on Si substrate and CRT cathode cap by low-pressure chemical vapor deposition. The CNTs consisted of multi-wall nanotubes (MWNTs) with an outer diameter range from 20 to 30 nm. The MWNTs emitter turns on at 2.2 V/μm and starts emitting 1 mA/cm^2 at 2.9 V/μm on the diode device. For practical display application, the fabricated CNTs electron gun was inserted into 19 in-sized CRT. We have investigated their long-term emission stability for 1000 h and demonstrated the window raster.

Keywords: Carbon nanotube; Field emission; Cathode ray tube

1. Introduction

Recently, carbon nanotubes (CNTs) have attracted considerable interest because of their unique physical properties and many potential applications [1,2]. Especially, due to their extreme aspect ratios, the CNTs feature large local field enhancement and thus yield considerable field emission currents at relatively low applied voltages. The CNTs have a strong potential to be applied to field emitters for superior emissive devices including flat panel displays, cathode-ray tubes backlight for liquid crystal displays, and outdoor displays [3,4]. In case of cathode ray tubes (CRT), the cathode is one of the most important components. Cathode current determines directly the brightness on image screen. Therefore, higher current density of cathode is dominantly required for higher brightness and higher definition. Long lifetime and high reliability for commercial applications are also required. The CNTs emitters satisfy above-mentioned requirements. Moreover, The CNTs cold cathode features low power consumption, rapidly turn on, and small thermal deformation of the electrodes. Though, there are still a few technical problems to be solved, the

*Corresponding author. Tel.: +82-2-958-5773; fax: +82-2-958-5692.
E-mail address: ytjang@kist.re.kr (Y.-T. Jang).

0042-207X/03/$ - see front matter
PII: S0042-207X(02)00290-7

CNTs electron emitter is a very promising candidate for the reliable electron guns for various applications including cathode ray tube [5].

In this work, we show the field emission properties of CNTs directly grown on Si substrate and conventional CRT cathode cap at low temperature ($<650^{\circ}C$) by thermal low-pressure chemical vapor deposition (LPCVD) method. In addition, in order to practical display application, we present fabrication of the CNT electron guns for the CRT and their electron emission properties as well as light emitting characteristics.

2. Experiment

The experiments were carried out in a thermal LPCVD system [6]. Fig. 1 shows the brief schematic of an experimental setup used for the growth of CNTs. We used the halogen lamp as a heat source, therefore it was possible to heat up and cool down rapidly to process temperature. Before the substrate was introduced into the reaction chamber, the catalytic metals with thickness of 10 nm were deposited on heavily doped-silicon substrate (0.001–0.002 Ω cm) and conventional cathode cap by rf magnetron sputtering. The substrates were loaded into the quartz reactor and pumped down by mechanical pump. After the reactor pressure reached below 10^{-3} Torr, N_2/H_2 were introduced into the reactor with heating up to 650°C. The typical flow rate of N_2 was 180 sccm and that of H_2 was 20 sccm. The heat treatment for making catalytic metal to nano-sized particles was conducted, and then the reactor pressure was kept at 10 Torr. After the working pressure had been stabilized, C_2H_2 instead of H_2 was introduced into the reactor for the CNTs growth. The CNTs were grown on catalytic particles by pyrolysis of C_2H_2.

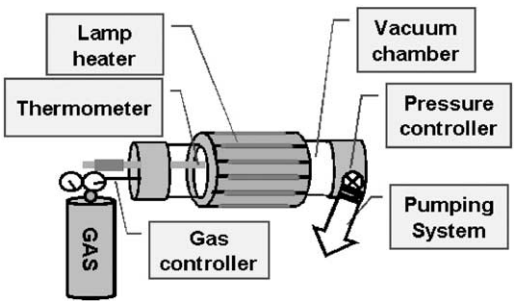

Fig. 1. The schematic diagram of the rapid thermal CVD experimental set-up.

To investigate the structures of CNTs, transmission electron microscopy (TEM) and high resolution scanning electron microscopy (HRSEM) were used. The field emission measurements were carried out in a vacuum camber at about 10^{-6} Torr. For I–V characteristics, an anode was placed directly above the CNTs using a 200 μm-thick spacer. A Keithley 237 source measure unit was used for sourcing the voltage and measuring the current.

Finally, we assembled the electron gun with CNTs cold cathode and made the CRT by conventional packaging method of CRT. After packaging, the field emission properties were investigated by the universal CRT test system (MECC Corp.).

3. Results and discussion

3.1. Characteristics of CNTs

Catalytic metal should be prepared in the form of droplets because the size of the round catalytic particles is a critical factor in CNTs formation by thermal CVD [7]. We tried previously to investigate the formation of the droplets at 650°C. Fig. 2 shows the SEM images of the droplets obtained by heat treatment of catalytic thin film with the original thickness of 10 nm at the time range from 10 to 30 min under N_2/H_2 ambient. Fig. 2a shows less separated grains with rectangular shape due to the insufficient annealing time for migrating of deposited atom or molecules. According to increase in the annealing time to 30 min, it is shown in Fig. 2b that the round-shape grains with the size of about 200 nm are distributed over the entire substrate. In case of Co–Ni double layer film shown in Fig. 2c, the most frequent diameter of nano-sized particles is about 300 nm in the condition of annealing at 650°C for 30 min. The difference of CNT diameter is due to the

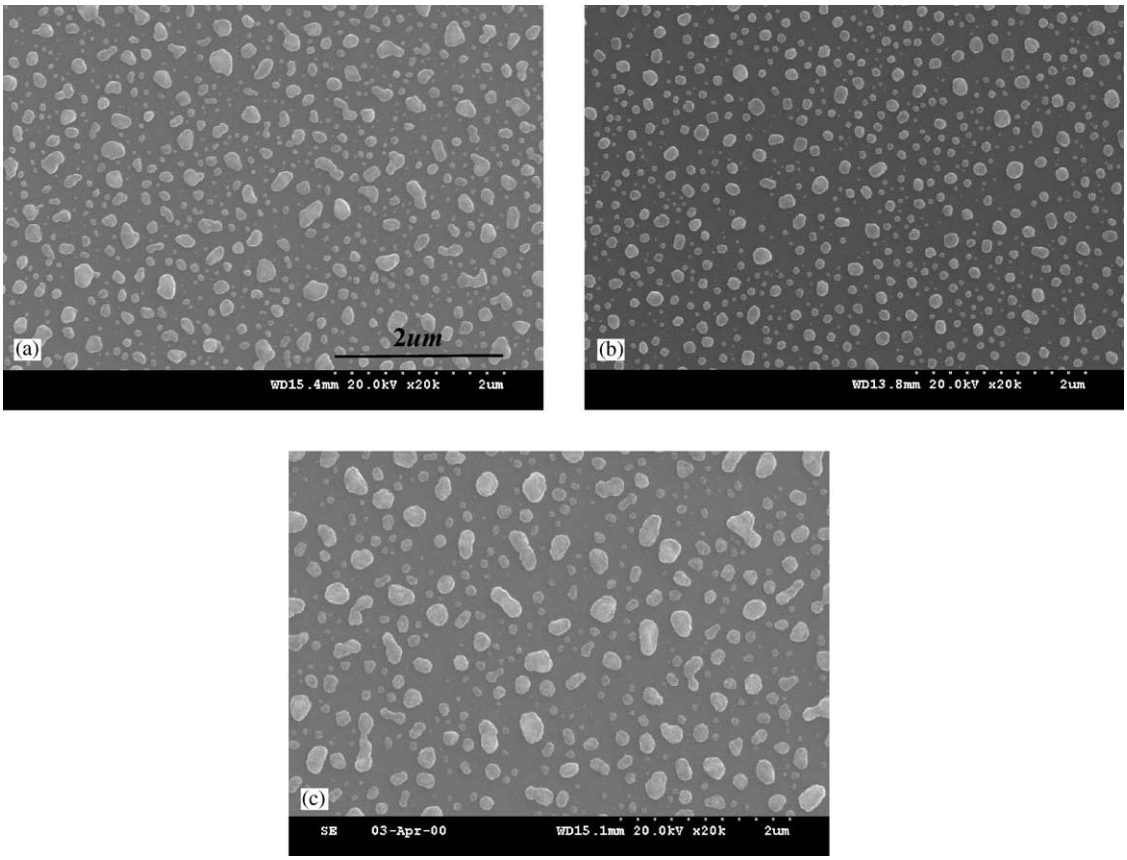

Fig. 2. SEM images of droplets obtained by heat treatment (a) Ni catalyst for 10 min (b) Ni catalyst for 30 min and (c) Ni–Co catalyst for 30 min.

differences of material properties such as the coefficient of thermal expansion, adhesion, etc.

Fig. 3a shows the HRSEM images of CNTs synthesized on droplet (see Fig. 2b) at 650°C under C_2H_2/N_2 ambient. The CNTs was grown with high density and had entangled and long noodle like shapes. We also observed some amorphous carbon layer and catalytic metal. The insert of Fig. 3a shows CNTs synthesized on Co–Ni droplet (see Fig. 2c). A considerable number of CNTs have a diameter of around 40 nm. The CNTs grown on smaller catalytic particles generally have smaller diameters and this fact indicates a strong correlation between the CNT diameter and the size of catalytic particles. TEM analysis was performed on the carbon nanotubes dispersed on a carbon TEM microgride after separating from the substrate by ultrasonic treatment in methanol. Fig. 3b is the TEM picture showing that CNTs were multiwall CNTs (MWNT) with an outer diameter range from 20 to 30 nm and consists of hollow compartments, looking like a bamboo and closed tip with no encapsulated particle.

Fig. 4 shows typical emission current density versus applied electric field characteristics for typical diode structure and the emission image through a phosphor-coated ITO glass. The dimension of CNTs films is $2 \times 2\,cm^2$. Fig. 4a shows the properties of CNTs synthesized on Ni particles. The field emission current of $1\,mA/cm^2$ was obtained at a field of $2.9\,V/\mu m$. This value is close to the reported field emission current for

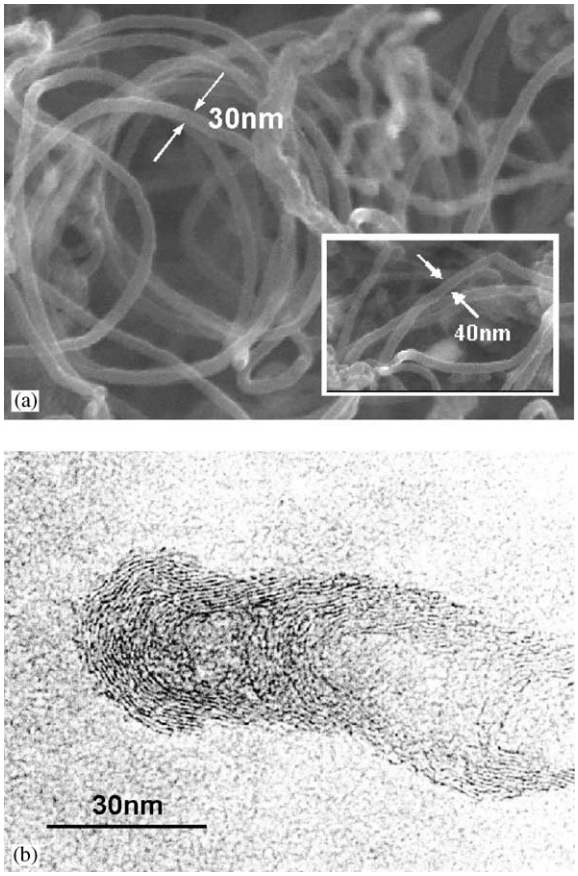

Fig. 3. (a) HRSEM image and (b) TEM image of CNTs grown on Ni nanodots under C_2H_2/N_2 ambient. Insert shows CNTs grown on Ni–Co catalyst.

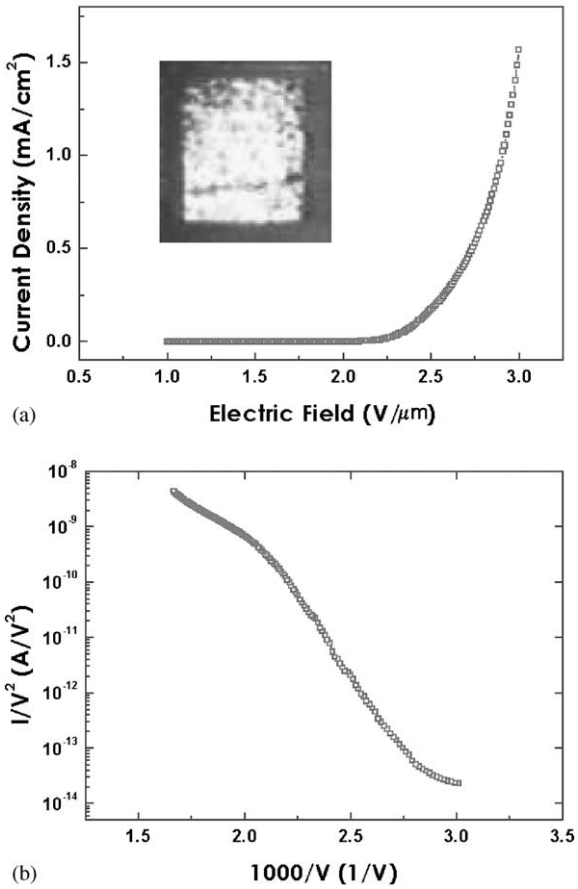

Fig. 4. (a) Field electron emission current density versus electrical field and (b) F–N plots for typical diode structure. Inset shows emission site density captured by charge coupled device camera.

well-aligned MWNT [8]. The result observed in diode structure suggests a sufficient possibility of using non-aligned CNT films as an efficient electron emitter [9]. The insert of Fig. 4a, typical images of the emission sites projected from ITO glass, indicates that the emission was dominated by a comparatively small number of very strong emitting sites spread out over the entire sample surface. Fig. 4b shows the Fowler–Nordheim plot for the CNTs. At low field region, we observed nearly straight line to indicate F–N behavior: $I = aE^2 \exp(-b/E)$, where a and b are constant and E is the electrical field strength at emitting point [10]. However, at high field region, the slope of F–N plot decreases, exhibiting a different emission behavior from that of the low field region. There is a controversy on this subject. In the case of a metal tip, deviations from F–N slope are usually attributed to space–charge effects. For CNTs, there are many reasons for deviations from F–N slope; the space–charge effect, interaction between neighboring nanotubes tips, and tip defects, and so on [11].

3.2. CNTs-CRT

We have made an electron emission gun for CRT with above-mentioned CNTs. Fig. 5a shows the photograph of cathode cap that is the same as

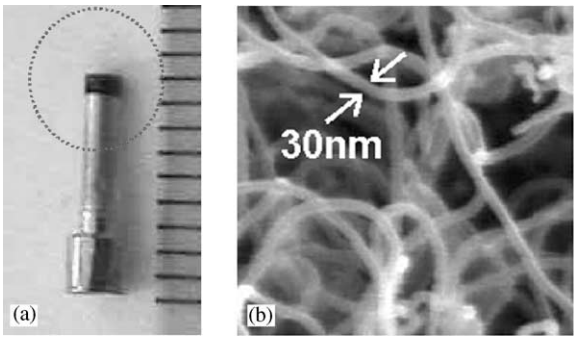

Fig. 5. (a) Photograph of conventional cathode cap and (b) HRSEM image of CNTs grown on cathode cap.

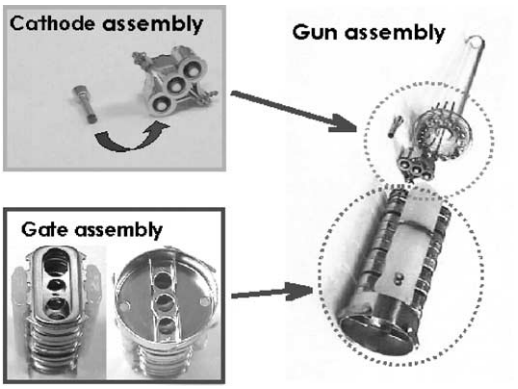

Fig. 6. Photograph of the electron gun assembly with CNTs cold cathode.

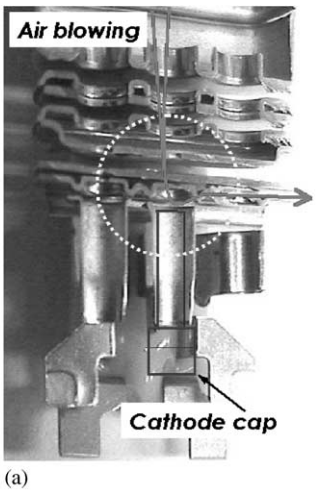

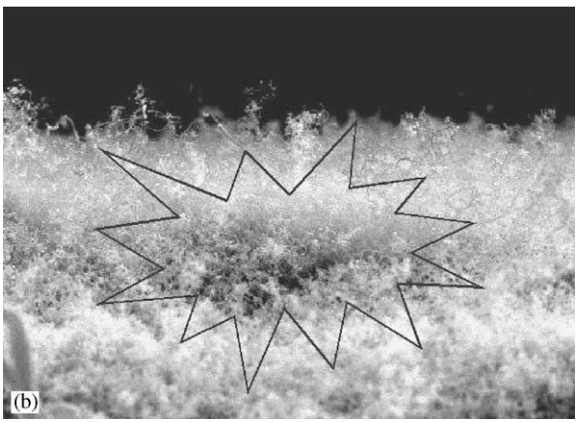

Fig. 7. (a) Cross-sectional view of electron gun assembly and (b) SEM image of CNT damaged during span-set process.

conventional thermionic cathode. The CNTs were directly grown on the top of cathode cap instead of thermionic emission materials. Fig 5b shows the HRSEM images of CNTs synthesized on Ni particles at 650°C under C_2H_2/N_2 ambient. The outer diameter range of these CNTs is from 30 to 40 nm. The difference of CNT diameter between Si substrate and cathode cap is due to the differences of surface roughness and adhesion.

Fig. 6 shows the electron gun assembly with CNTs cold cathode. The structure of the main lens is the same as that of thermionic cathode electron gun. CNTs were directly grown on cathode cap, which were mounted gun assembly. As-grown CNTs are used without post-purifying treatment. The thermionic cathode is simply replaced by CNTs cold cathode without additional process. For uniform focusing over screen, multi-step focusing structure is adopted.

Fig. 7a shows the schematic cross-sectional view of electron gun assembly during span-set process. The span-set process is to adjust distance between cathode cap and gate electrode by air pressure. Sometimes CNTs partially contact with gate electrode due to non-uniformity of length. The strong air blowing also caused the damage to directly grown CNTs as shown in Fig. 7b. It is necessary to control the uniformity of length and

to improve the adhesion of CNTs. In our experimental, the adhesion on substrate and the resistance against strong blowing of non-aligned CNTs were better than those of aligned CNTs because CNTs were entangled.

We have made the CNTs cold cathode CRT using the conventional packing method of CRT. The CNTs electron gun assembly was mounted into CRT bulb and neck glass was sealed under vacuum. The pressure of CRT tube was 5×10^{-6} Torr. The Universal CRT test system (MECC Corp.) was employed for analyzing the electron emission characteristics and the performance of the CNTs-CRT.

Fig. 8a shows long-term emission stability under constant applied field after packaging. V_{anode}, V_{G3}, V_{G2}, V_{G1}, and $V_{cathode}$ were biased at 27, 7, 1.6, and 1.1 kV, and grounded, respectively, as shown in insert of Fig. 8a. The current in Fig. 8a was the anode current, which was measured at phosphor screen of CRT. The gap distance between the cathode and anode was 100 μm. There was little degradation of emission current and however, no arcing in the beginning stage. After the short-term aging a current increase was observed and also a stabilized current characteristics was resulted. The electron gun showed the problem such a considerable leakage current between the gate and emitter electrodes. Until now, it is hard to control uniform potential distribution between the edge and the center of cathode due to using the conventional gun assembly that has circular hole electrodes. At the next works, we will start to optimize the gate structure for improving the emission current and the gate leakage current. As shown in Fig. 8b, the window raster pattern in a 19-in CRT screen was demonstrated with only one electron gun (green) under above-mentioned applied voltage. Because the bulk tube without anti-reflection coating layer was used for the cold cathode-CRT sample, there are some reflections in this figure. Future work is needed for display action with three CNTs cathode.

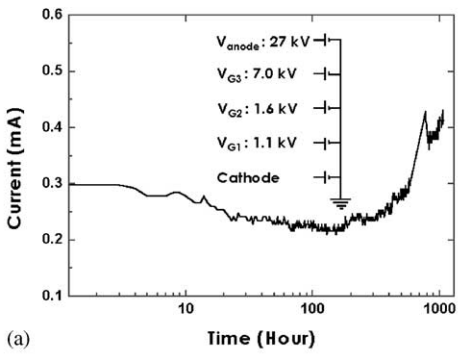

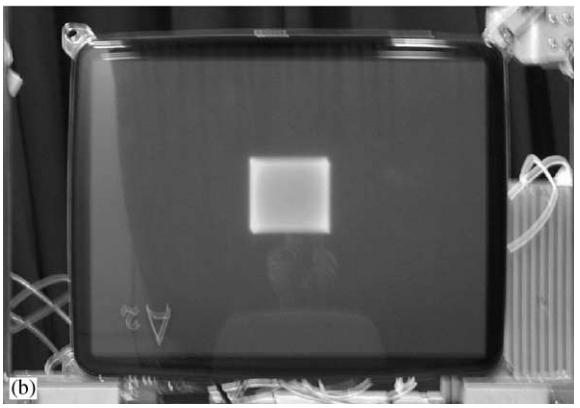

Fig. 8. (a) Temporal variation of emission current at constant applied voltage and (b) window raster pattern achieved by our CNTs-CRT.

4. Summary

In the present work, we have successfully grown the CNTs on Si substrate and conventional cathode cap of CRT by rapid thermal chemical vapor deposition using C_2H_2 gas at 650°C. The CNTs showed a low turn-on voltage and high emission current. We simply replaced a thermionic cathode with CNTs cold cathode and then confirmed a long-term field emission stability. Finally, we demonstrated the window raster pattern in a 19-in screen. Though there are a few technical problems to be solved, the CNTs were successfully applied to cold cathode as an electron source of CRT.

References

[1] Iijima S. Nature 1991;354:56.
[2] Iijima S, Ichihashi T. Nature 1993;363:606.

[3] Kuttel O, et al. Appl Phys Lett 1998;73:2113.
[4] Bonard JJM, Salvetat J-P, Stockli T, Forro L, Chatelain A. Electrochem Soc Proc 1998;Col. 98-8:783.
[5] Uemura S, Nagasako T, Yotani J, Shimojo T, Saito Y. Proceedings of the SID '98 Dig. 1998. p. 105.
[6] Lee CJ, Park J. Appl Phys Lett 2000;77:3397.
[7] Yudasaka M, et al. Appl Phys Lett 1997;70(14):1817.
[8] Saito Y, Hamaguchi K, Uemura S, Uchida K, Tasaka Y, Ikazaki F, Yumura M, Kasuya A, Nishina Y. Appl Phys A 1998;67(1):95.
[9] Chen Y, Shaw DT, Guo L. Appl Phys Lett 2000;76(17):2469.
[10] de Heer WA, et al. Adv Mater 1997;9(1):87.
[11] Collins PG, Zettl A. Phys Rev B 1997;55:9391.